ACS APPLIED MATERIALS & INTERFACES

Research Article

www.acsami.org

Inhibiting the VIM-2 Metallo-β-Lactamase by Graphene Oxide and Carbon Nanotubes

Po-Jung Jimmy Huang, Rachel Pautler, Jenitta Shanmugaraj, Geneviève Labbé, and Juewen Liu*

Department of Chemistry, Waterloo Institute for Nanotechnology University of Waterloo, Waterloo, Ontario, Canada N2L 3G1

Supporting Information

ABSTRACT: Metallo-β-lactamases (MBLs) degrade a broad spectrum of antibiotics including the latest carbapenems. So far, limited success has been achieved in developing its inhibitors using small organic molecules. VIM-2 is one of the most studied and important MBLs. In this work, we screened 10 nanomaterials, covering a diverse range of surface properties including charge, hydrophobicity, and specific chemical bonding. Among these, graphene oxide and carbon nanotubes are the most potent inhibitors, while most other materials do not show much inhibition effect. The inhibition is noncompetitive and is attributed to the hydrophobic interaction with the enzyme. Adsorption of VIM-2 was further probed using protein displacement assays where it cannot displace or be displaced by bovine serum albumin (BSA). This information is useful for rational design inhibitors for MBLs and more specific inhibition might be achieved by further surface modifications on these nanocarbons.

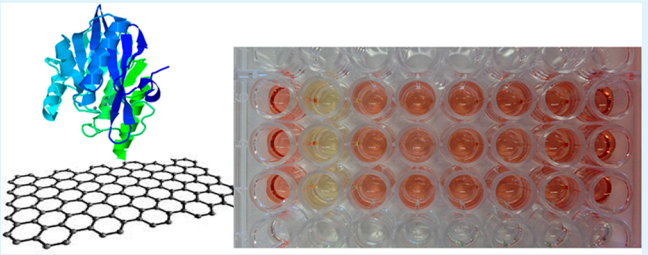

KEYWORDS: *graphene, beta-lactamases, inhibition, adsorption, carbon nanotubes, nanomaterials*

INTRODUCTION

Many life-saving antibiotics are based on β-lactams that inhibit the synthesis of bacterial cell walls. The efficacy of such antibiotics, however, has been declining in the past few decades because bacteria constantly evolve enzymes known as β-lactamases that hydrolyze β-lactam antibiotics.[1] Developing inhibitors is a common strategy to combat β-lactamases. These are compounds that bind tightly to the enzyme active site without being hydrolyzed or released. Finding appropriate inhibitors has been extremely challenging; in the past few decades, only a few inhibitors have been approved for clinical use.[2]

Over the years, a few classes of β-lactamases have been identified on the basis of the structure of their active sites. Metallo-β-lactamases (MBLs) belong to Class B, according to the enzyme structure classification.[3] MBLs are particularly detrimental because they degrade a broad spectrum of antibiotics including the latest carbapenems.[4] At the same time, they cannot be inhibited by the current β-lactamase inhibitors. VIM-2 is a subclass B1 MBL showing Zn^{2+}-dependent activity.[5] It has a molecular weight of 25515 Da and a monomeric structure.[6] Since early 2000s, VIM-2 has been one of the most reported MBL worldwide and is thus the primary target for developing inhibitors for MBLs.

While most efforts in this field have been devoted to the synthesis of small organic molecules, in the past 30 years, significant progress has been made in nanomaterials synthesis and application. In particular, nanomaterials have been interfaced with enzymes through a number of different mechanisms.[7,8] First, a few nanomaterials were found to have enzyme-like activities and, thus, are explored as enzyme mimics. The best examples are the use of gold nanoparticles as both a glucose oxidase mimic[9−11] and a nuclease mimic,[12] cerium oxide nanoparticles as a general oxidase mimic,[13] and iron oxide nanoparticles as a peroxidase mimic.[14,15] Second, some nanomaterials can stabilize enzymes. For example, Zare and co-workers reported templated formation of copper phosphate nanoflowers in the presence of proteins and the embedded lactase showed much higher stability.[16] Wang et al. recently reported that α-amylase activity is significantly boosted by calcium phosphate nanoparticles because the enzyme can more stably bind Ca^{2+} within the nanoparticle.[17] Finally, nanomaterials can also act as enzyme inhibitors. In particular, graphene oxide (GO) has been reported to be an inhibitor for a few enzymes including α-chymotrypsin[18] and β-galactosidase.[19] On the other hand, PEGylated GO can boost the activity of trypsin but has no effect on chymotrypsin or proteinase K, which are also serine proteases.[20]

Given the vast number of nanoparticles with diverse surface properties, new insights may be obtained by studying the interaction between enzymes and nanoparticles. For example, we may probe electrostatic interaction, hydrophobic interaction, and specific chemical bonding by changing the surface ligands of nanoparticles.[21,22] Although nanomaterial-based inhibitors are unlikely to be directly useful in clinical settings due to unknown safety and delivery related issues, such

Received: March 5, 2015
Accepted: April 21, 2015
Published: April 21, 2015

DOI: 10.1021/acsami.5b01954
ACS Appl. Mater. Interfaces 2015, 7, 9898−9903

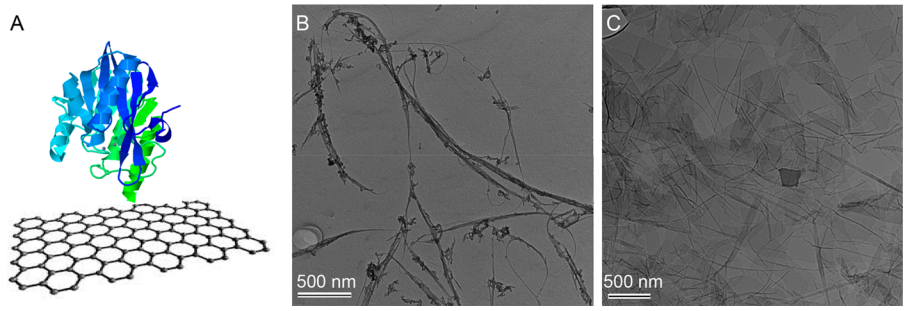

Figure 1. (A) Schematics of VIM-2 adsorption by graphene. The protein structure was exported from the structure viewer of Protein Data Bank based on the data from reference.[23] TEM micrographs of (B) CNT and (C) GO used in this work.

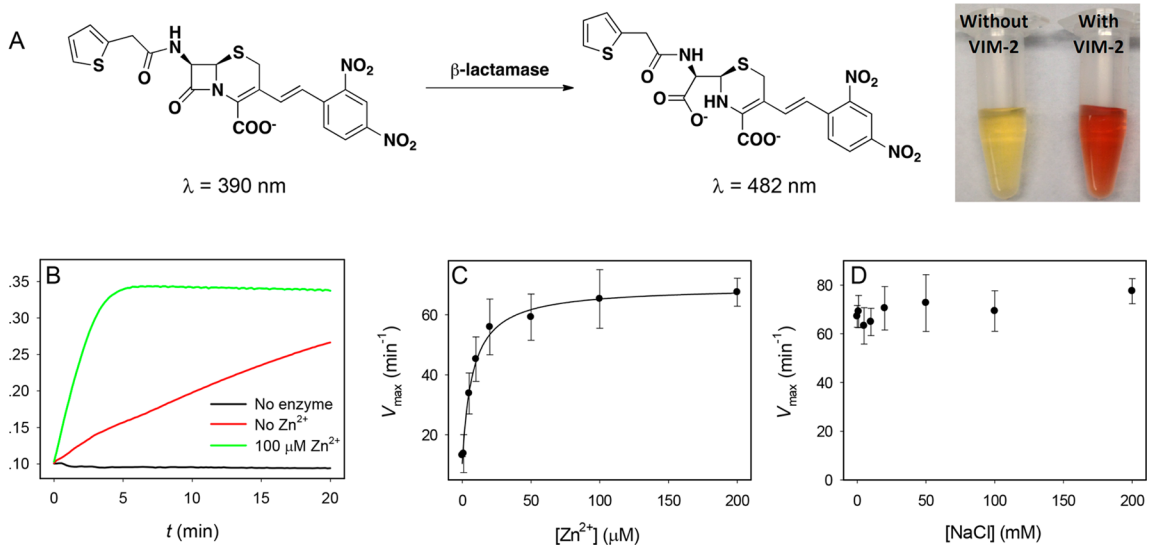

Figure 2. (A) Chemical reaction of nitrocefin hydrolysis and photograph showing its color change before and after hydrolysis. (B) Kinetics of the color change in the absence and presence of VIM-2 and the effect of Zn^{2+}. Effect of (C) Zn^{2+} concentration and (D) NaCl concentration on the activity of VIM-2.

research might identify appropriate surfaces for enzyme immobilization and spark ideas for a rational design of new inhibitors. Herein, we screened a number of nanomaterials as VIM-2 inhibitors, where a few sp^2 nanocarbons were found to be quite potent.

MATERIALS AND METHODS

Chemicals. LB broth EZMix powder, sodium chloride, zinc chloride, zinc sulfate, bovine serum albumin (BSA), and Triton X-100 were purchased from Sigma-Aldrich. Acrylamide/bis(acrylamide) solution (29:1), 10× TBE, coomassie brilliant blue R-250, and kanamycin sulfate were purchase from Bio Basic, Inc. (Ont, Canada). Nitrocefin was purchased from TOKU-E (Bellingham, WA). HEPES-free acid, HEPES, and sodium salt were purchased from Amresco. Graphene oxide was purchased from ACS Material (Medform, MA). All the lipids were from Avanti Polar Lipids, Inc. CeO_2 was from Sigma-Aldrich. Milli-Q water was used to prepare all the buffers and solutions.

VIM-2 Expression and Purification. The VIM-2 gene was amplified from pNOR-2001,[5] (generous gift from P. Nordmann) using the following PCR primers: (5′-GGGTTTCCATGGGCATGTTCA-AACTTTTGAGTAAG; 5′-AGTACCGAATTCCTACTCAAC-GACTGAGCG. The VIM-2 gene was subcloned into the NcoI-EcoRI sites of pET28a. The plasmid was transformed into *Escherichia coli* BL21, which was grown overnight in 4 L TB medium supplemented with 40 μg/mL kanamycin. The enzyme was purified from 30 g of cells harvested by centrifugation at 6,300*g*. The cells were resuspended in 170 mL of buffer A (50 mM MES buffer, pH 6.5, 10 μM $ZnCl_2$), supplemented with 20 mg of lysozyme and 1 mg of DNase I. The cells were disrupted by 2 passages in a homogenizer at 17 000 psi. The cell debris was removed from the lysate by centrifugation at 48 000*g* for 30 min at 4 °C. The crude extract (155 mL) was loaded at 2.5 mL/min on a Sepharose-Q fast flow column (30 mL bed volume) pre-equilibrated with buffer A. The column was washed with 10 CV of buffer A, until OD_{280} = 0.1. The enzyme was eluted with a salt gradient from 0 to 300 mM NaCl over 10 CV, at a flow rate of 2 mL/min. The active fractions were pooled, and the protein was concentrated with a 50 mL Amicon concentrator fitted with a YM-10 membrane (10 kDa cutoff). The protein was then injected on a Superdex 200 HiLoad 26/60 column equilibrated with 50 mM sodium phosphate buffer, pH 7.0, 0.3 M NaCl, and 2 μM $ZnSO_4$ and the eluent was collected in 3 mL fractions. The most active fractions were pooled, and aliquots were flash-frozen in liquid nitrogen and stored at −80 °C. Protein concentration was determined using the Bradford method.

Nitrocefin Assay. In a typical assay, a VIM-2 stock solution was diluted in buffer B (50 mM HEPES buffer pH 7.3, 100 μM $ZnCl_2$). Assays were performed at room temperature (~25 °C). The final VIM-2 concentration was 12.5 ng/mL in the presence of 100 μM nitrocefin. The appearance of the hydrolysis product of nitrocefin was monitored at 482 nm. Enzyme kinetic values were calculated based on a coefficient of extinction of 17 400 M^{-1} cm^{-1} at 482 nm for the hydrolysis product.

Circular Dichroism (CD) Spectroscopy. CD measurement was carried out on a JASCO 700 instrument. To decrease noise in the CD spectra, we diluted VIM-2 in 10 mM phosphate buffer, pH 7.3 containing 100 μM $ZnCl_2$. The final VIM-2 concentration was 0.2 mg/

DOI: 10.1021/acsami.5b01954
ACS Appl. Mater. Interfaces 2015, 7, 9898−9903

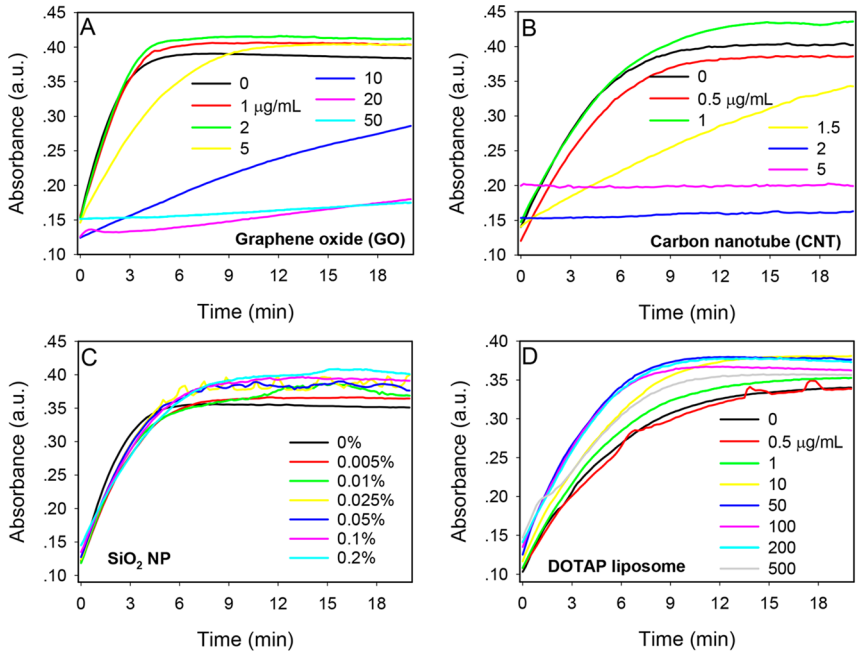

Figure 3. Kinetics of nitrocefin color change induced by VIM-2 in the presence of various concentrations of nanomaterials: (A) GO, (B) CNT, (C) 50 nm SiO_2 NPs, and (D) cationic DOTAP liposomes.

mL. To this sample, 5 μL of 25 mg/mL GO was added for each addition, increasing the GO concentration by 250 μg/mL each time to a maximum of 1 mg/mL. Above this point, the signal could not be clearly determined due to a large increase in noise. CD spectra for each GO concentration were obtained at room temperature with and without protein.

RESULTS AND DISCUSSION

Zn^{2+}-Dependent VIM-2. In this work, we study the adsorption of VIM-2 by nanomaterials. A scheme of VIM-2 adsorption by graphene is shown in Figure 1A. VIM-2 is a Zn^{2+}-dependent enzyme. We purified VIM-2 following established procedures.[5] Before studying the effect of nanomaterials, we optimized the assay conditions. Using nitrocefin as the chromogenic substrate (Figure 2A), we studied the effect of Zn^{2+} concentration on enzyme activity. In a typical reaction, the VIM-2 concentration was 42 nM and the nitrocefin concentration was 100 μM. When saturated with Zn^{2+}, the enzyme has a turnover number of ~40 s^{-1}. Figure 2B shows a typical kinetic assay using nitrocefin without and with 100 μM additional Zn^{2+}. The rate difference is ~7-fold. Next, the enzyme rate (V_{max}) is plotted as a function of Zn^{2+} concentration (Figure 2C), where an apparent dissociation constant (K_d) of 7.4 μM for Zn^{2+} is obtained. This Zn^{2+} binding affinity is similar to the literature reported values.[24] The enzyme activity reached a plateau at a concentration of 100 μM Zn^{2+}, which was used in subsequent studies. Because salt concentration is important for tuning the interaction with nanomaterials, we next studied the effect of ionic strength. Interestingly, VIM-2 activity appears independent of the NaCl concentration from 0 to 200 mM (Figure 2D). These basic understandings allow us to further explore the properties of VIM-2 in the presence of various nanomaterials.

Nanomaterials as Inhibitors. Since VIM-2 is a negatively charged protein, we suspect that cationic nanoparticles might be inhibitors based on electrostatic interactions. In addition, proteins generally contain a hydrophobic core, which might be disturbed by using hydrophobic materials. Finally, certain amino acids contain surface reactive groups, such as thiol and amine that might have affinity for metal surfaces. To have a systematic understanding, we performed enzyme activity assays in the presence of various nanomaterials. For each material, VIM-2 activity was measured as a function of materials concentration. For example, graphene oxide (GO) strongly inhibited VIM-2 and a typical set of response curves are shown in Figure 3A. A dose-dependent inhibition was observed, and significant inhibition was achieved with 20 μg/mL GO. Carbon nanotubes (CNTs) inhibited VIM-2 even more strongly, and complete inhibition was achieved at just 2 μg/mL. Both GO and CNTs contain hydrophobic regions and are negatively charged due to the surface carboxyl groups. The elevated baseline at high nanomaterials concentration was due to light absorption or scattering by these materials. On the other hand, neither negatively charged SiO_2 nanoparticles (Figure 3C) nor positively charged DOTAP liposomes (Figure 3D) inhibited VIM-2, even at very high concentrations. Therefore, surface charge does not appear to play an obvious role while hydrophobicity is more important. The TEM micrographs of GO and CNT used in this work are shown in Figure 1B,C. The characterization of other nanomaterials has been reported in our previous publications[25−27] and in the Supporting Information (Figures S1 and S2).

To have a complete understanding, we tested six more nanomaterials using the same method. A representative data point at a high nanomaterial concentration was selected and we plotted the inhibition effects of all these nanomaterials (Figure 4). The x axis is the concentration tested, and the y axis is the percentage of activity inhibition at that nanomaterial concentration. Therefore, the most potent inhibitors are at the top left corner, where CNT and GO are located. Although nanodiamond is also a type of nanocarbon, it is not an inhibitor. This might be related to its sp^3 nature, while CNT and GO contain mainly sp^2 carbons. Therefore, $\pi-\pi$ stacking might also be important. A close look at the enzyme active site reveals three histidine residues for Zn^{2+} coordination. Interaction of

DOI: 10.1021/acsami.5b01954
ACS Appl. Mater. Interfaces 2015, 7, 9898−9903

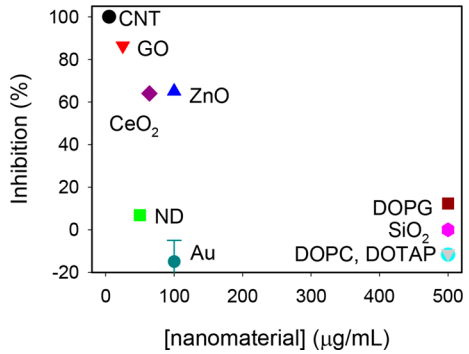

Figure 4. Inhibition of VIM-2 by various nanomaterials at their highest tested concentrations. The most potent inhibitors are in the top left corner.

these residues with sp^2 carbons might be a reason for the inhibition. Data from X-ray crystallography and mutagenesis have also established the importance of the hydrophobic core at the active site.[28,29]

We did not observe any inhibition with gold nanoparticles (AuNPs), which can bind to exposed cysteine, methionine, and lysine residues. In the crystal structure, Cys221 uses its thiol group for Zn^{2+} binding, but this residue is buried deeper in the active site and might not be accessible by AuNPs. This work also suggests that AuNPs or other gold surfaces might be useful for VIM-2 immobilization if its activity needs to be maintained. We also tested a number of oxides. Only ZnO and CeO_2 showed moderate inhibition, while SiO_2 was not inhibitory. To systematically test the effect of charge, we employed cationic DOTAP, anionic DOPG and zwitterionic DOPC liposomes. VIM-2 remained active in all these liposomes. Based on our data, hydrophobicity and potentially aromatic stacking are the most important factors for inhibiting VIM-2.

Probing Enzyme Adsorption. Because GO and CNT are the most potent inhibitors and share similar properties, we next studied them in more detail in terms of adsorption. First, the effect of NaCl was studied to probe electrostatic interactions. The free enzyme remains active, even in the absence of NaCl (black trace, Figure 5A). However, we did not observe much inhibition with the addition of GO (50 μg/mL) in the absence of NaCl (red curve). Stronger inhibition was achieved with increasing concentrations of NaCl, and the effect was saturated with >100 mM NaCl. From Figure 2D, we know that the VIM-2 activity is independent of NaCl concentration. Therefore, the effect of NaCl in Figure 5A must be due to VIM-2/GO interactions. Because both VIM-2 and GO are negatively charged, VIM-2 cannot be adsorbed by GO at low salt due to charge repulsion. This experiment supports that inhibition is due to adsorption of VIM-2 by GO.

Next, we probed adsorption strength using BSA. When CNTs were incubated with BSA before adding VIM-2, the VIM-2 activity was fully retained as long as the BSA concentration was higher than 1 μg/mL (Figure 5B). On the other hand, when VIM-2 and CNT were mixed first, BSA cannot rescue the activity even at very high protein concentrations (Figure 5C). This study further confirms that protein adsorption is the first step of inhibition. In addition, VIM-2 adsorption appears to be quite stable and cannot easily be displaced by other proteins.

Inhibition Mechanism. An enzyme inhibitor can act via a few different mechanisms. To study this, we measured VIM-2 activity in various concentrations of the nitrocefin substrate and in different GO concentrations (Figure 6A). The initial enzyme velocity curves for different substrate concentrations drop with an increasing concentration of GO. The mode of inhibition is determined through a Lineweaver–Burk plot (Figure 6B). These lines do not cross the y axis at the same point, and thus the mechanism is noncompetitive inhibition (GO does not compete for the substrate binding site). In fact, this pattern indicates a strong noncompetitive inhibition. This mechanism is different from GO inhibition of α-chymotrypsin, where the mechanism was determined to be competitive.[18]

Circular dichromism (CD) spectroscopy was used to investigate the effect of GO on the secondary structure of VIM-2. In this experiment, GO was added to a VIM-2 sample and the CD spectrum was recorded after each addition. Before any GO additions, VIM-2 shows peaks at 210 and 220 nm (Figure 7), indicating a large fraction of α-helical structure, which is consistent with its crystal structure.[6] With the addition of GO, the peak locations do not change, indicating that VIM-2 adsorption by GO does not disrupt its global structure. However, the peak intensity decreases as the concentration of GO increases, indicating that the enzyme locally loses its alpha helical structure. This is consistent with the noncompetitive inhibition mechanism.

Further Discussion. Studying the interaction between nanomaterials and proteins is important for drug delivery, toxicology, and biosensor development. Depending on the surface chemistry of both proteins and nanomaterials, they can have a diverse range of interactions.[30] A number of previous works have focused on using monolayer-functionalized AuNPs, where the surface chemistry can be systematically controlled.

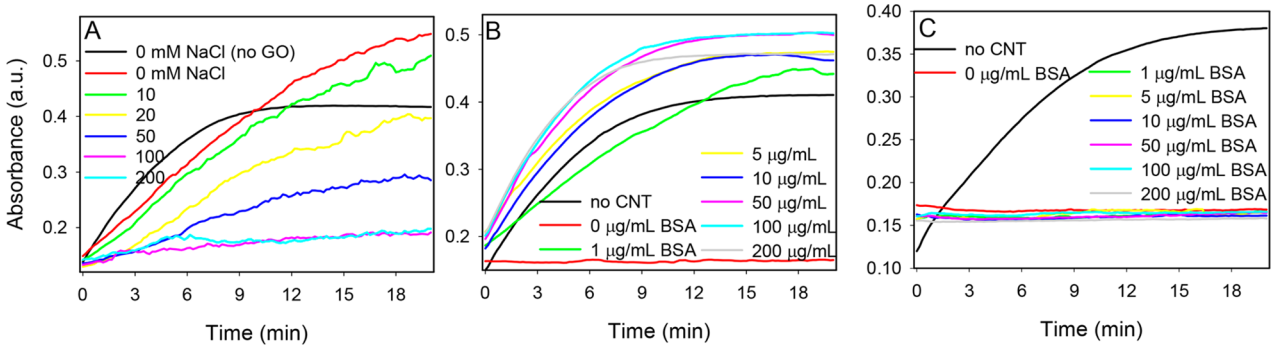

Figure 5. (A) Effect of NaCl on GO-induced inhibition of VIM-2. (B) Mixing BSA and CNT first followed by adding VIM-2 can reduce the inhibition effect. (C) The enzyme activity cannot be rescued by the addition of BSA, after VIM-2 is mixed with CNT.

DOI: 10.1021/acsami.5b01954
ACS Appl. Mater. Interfaces 2015, 7, 9898–9903

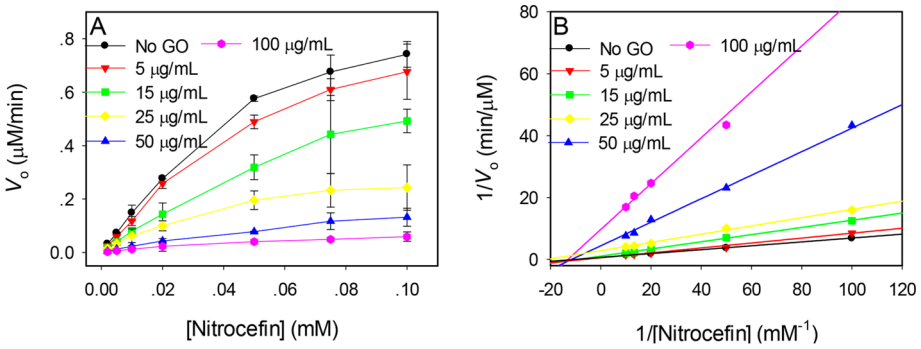

Figure 6. (A) Enzyme velocity as a function of nitrocefin concentration at various GO concentrations. (B) Lineweaver–Burk plot of the same data indicating noncompetitive inhibition.

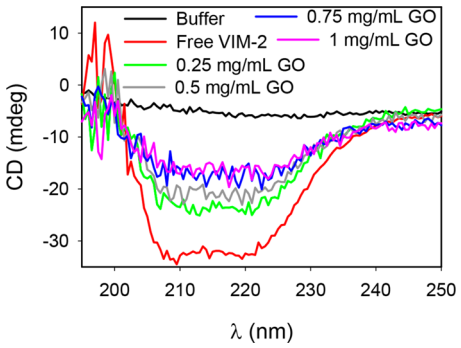

Figure 7. CD spectra of VIM-2 in the presence of various concentrations of GO.

Changing the core material as shown in this work provides an alternative method where different surface properties can also be easily accessed. It must be noted that GO interacts with proteins through different mechanisms.[31] In the case of VIM-2 case, hydrophobic interaction and $\pi-\pi$ stacking appears to be crucial.

CNT, graphene, and GO have been interfaced with various biological systems including lipid membranes,[32−35] nucleic acids,[36−38] proteins,[18,19] and cells.[39,40] In most cases, hydrophobic interaction appears to be quite important. From this study, we know that VIM-2 is more easily inhibited by hydrophobic surfaces containing sp^2 carbons. Both planar GO and rod-like CNT can achieve the inhibition effect. This knowledge might be useful for the rational design of small molecule based inhibitors. When GO and CNT are compared, the latter is about 10-fold more potent. Because CNTs have very small diameters, it might better fit the hydrophobic enzyme pocket, and thus, its surface is more efficiently utilized. We achieved full inhibition with 2 μg/mL of CNT, where the VIM-2 concentration was only 12.5 ng/mL. Therefore, it is unlikely that all the surface area of CNTs was utilized, possibly due to aggregation of the materials. Future work will focus on rational modification of nanomaterials with the goal of achieving highly potent and specific inhibition effect.

While GO and CNT are potent inhibitors for VIM-2, it is unlikely that they can be directly used clinically for the following reasons. First, the BSA adsorption study indicates that the surface of GO and CNT can be easily blocked by other proteins. Once that happens, VIM-2 cannot be adsorbed or inhibited. Given the extremely high concentration of proteins in both culture medium and inside cells, it is unlikely that VIM-2 can be selectively adsorbed. Second, VIM-2 mainly exists as an intracellular enzyme (even though it can also be released to the surrounding medium). To effectively inhibit VIM-2 in live cells, the nanomaterials need to cross the cell membrane, which is a major challenge in the development of antibacterial agents. Finally, the safety issue of nanomaterials need to be addressed before clinical administration. For these reasons, the main goal of this work is to probe the property of VIM-2 using nanomaterials, and such understanding may be used to guide rational design of small molecule based inhibitors.

CONCLUSIONS

In summary, we have screened a diverse range of nanomaterials as inhibitors for an important MBL: VIM-2. Among these, GO and CNTs appeared to be the most potent inhibitors, highlighting the importance of hydrophobic interactions. The inhibition mechanism is noncompetitive, which is likely due to local denaturation of the enzyme on the surface of the nanomaterials upon adsorption. Controlling the surface chemistry of nanomaterials might further improve their inhibition effects. This information is useful for guiding rational design of VIM-2 inhibitors.

ASSOCIATED CONTENT

Supporting Information

DLS spectra of liposomes and TEM micrographs of SiO_2 and ZnO nanoparticles used in this work. The Supporting Information is available free of charge on the ACS Publications website at DOI: 10.1021/acsami.5b01954.

AUTHOR INFORMATION

Corresponding Author

*Fax: (+1) 519-746-0435 E-mail: liujw@uwaterloo.ca.

Notes

The authors declare no competing financial interest.

ACKNOWLEDGMENTS

This work is supported by the Canadian Institutes of Health Research (CIHR) through a Canada–UK team grant, and by the Natural Sciences and Engineering Research Council of Canada (NSERC).

REFERENCES

(1) Taubes, G. The Bacteria Fight Back. *Science* **2008**, *321*, 356–361.
(2) Drawz, S. M.; Bonomo, R. A. Three Decades of Beta-Lactamase Inhibitors. *Clin. Microbiol. Rev.* **2010**, *23*, 160–201.
(3) Bush, K.; Jacoby, G. A. Updated Functional Classification of β-Lactamases. *Antimicrob. Agents Chemother.* **2010**, *54*, 969–976.

DOI: 10.1021/acsami.5b01954
ACS Appl. Mater. Interfaces 2015, 7, 9898–9903

(4) Cornaglia, G.; Giamarellou, H.; Rossolini, G. M. Metallo-β-Lactamases: A Last Frontier for β-Lactams? *Lancet Infect. Dis.* **2011**, *11*, 381−393.
(5) Poirel, L.; Naas, T.; Nicolas, D.; Collet, L.; Bellais, S.; Cavallo, J. D.; Nordmann, P. Characterization of VIM-2, a Carbapenem-Hydrolyzing Metallo-Beta-Lactamase and Its Plasmid- and Integron-Borne Gene from a Pseudomonas Aeruginosa Clinical Isolate in France. *Antimicrob. Agents Chemother.* **2000**, *44*, 891−897.
(6) Garcia-Saez, I.; Docquier, J. D.; Rossolini, G. M.; Dideberg, O. The Three-Dimensional Structure of VIM-2, a Zn-β-Lactamase from Pseudomonas Aeruginosa in Its Reduced and Oxidised Form. *J. Mol. Biol.* **2008**, *375*, 604−611.
(7) Kotov, N. A. Inorganic Nanoparticles as Protein Mimics. *Science* **2010**, *330*, 188−189.
(8) Wu, Z.; Zhang, B.; Yan, B. Regulation of Enzyme Activity through Interactions with Nanoparticles. *Int. J. Mol. Sci.* **2009**, *10*, 4198−4209.
(9) Comotti, M.; Della Pina, C.; Matarrese, R.; Rossi, M. The Catalytic Activity of "Naked" Gold Particles. *Angew. Chem., Int. Ed.* **2004**, *43*, 5812−5815.
(10) Zheng, X.; Liu, Q.; Jing, C.; Li, Y.; Li, D.; Luo, W.; Wen, Y.; He, Y.; Huang, Q.; Long, Y.-T.; Fan, C. Catalytic Gold Nanoparticles for Nanoplasmonic Detection of DNA Hybridization. *Angew. Chem., Int. Ed.* **2011**, *50*, 11994−11998.
(11) Luo, W.; Zhu, C.; Su, S.; Li, D.; He, Y.; Huang, Q.; Fan, C. Self-Catalyzed, Self-Limiting Growth of Glucose Oxidase-Mimicking Gold Nanoparticles. *ACS Nano* **2010**, *4*, 7451−7458.
(12) Manea, F.; Houillon, F. B.; Pasquato, L.; Scrimin, P. Nanozymes: Gold-Nanoparticle-Based Transphosphorylation Catalysts. *Angew. Chem., Int. Ed.* **2004**, *43*, 6165−6169.
(13) Asati, A.; Santra, S.; Kaittanis, C.; Nath, S.; Perez, J. M. Oxidase-Like Activity of Polymer-Coated Cerium Oxide Nanoparticles. *Angew. Chem., Int. Ed.* **2009**, *48*, 2308−2312.
(14) Gao, L.; Zhuang, J.; Nie, L.; Zhang, J.; Zhang, Y.; Gu, N.; Wang, T.; Feng, J.; Yang, D.; Perrett, S.; Yan, X. Intrinsic Peroxidase-Like Activity of Ferromagnetic Nanoparticles. *Nat. Nanotechnol.* **2007**, *2*, 577−583.
(15) Li, X.; Wen, F.; Creran, B.; Jeong, Y.; Zhang, X.; Rotello, V. M. Colorimetric Protein Sensing Using Catalytically Amplified Sensor Arrays. *Small* **2012**, *8*, 3589−3592.
(16) Ge, J.; Lei, J. D.; Zare, R. N. Protein-Inorganic Hybrid Nanoflowers. *Nat. Nanotechnol.* **2012**, *7*, 428−432.
(17) Wang, L. B.; Wang, Y. C.; He, R.; Zhuang, A.; Wang, X. P.; Zeng, J.; Hou, J. G. A New Nanobiocatalytic System Based on Allosteric Effect with Dramatically Enhanced Enzymatic Performance. *J. Am. Chem. Soc.* **2013**, *135*, 1272−1275.
(18) De, M.; Chou, S. S.; Dravid, V. P. Graphene Oxide as an Enzyme Inhibitor: Modulation of Activity of Alpha-Chymotrypsin. *J. Am. Chem. Soc.* **2011**, *133*, 17524−17527.
(19) Li, J.; Wu, L.-J.; Guo, S.-S.; Fu, H.-E.; Chen, G.-N.; Yang, H.-H. Simple Colorimetric Bacterial Detection and High-Throughput Drug Screening Based on a Graphene-Enzyme Complex. *Nanoscale* **2013**, *5*, 619−623.
(20) Jin, L.; Yang, K.; Yao, K.; Zhang, S.; Tao, H.; Lee, S.-T.; Liu, Z.; Peng, R. Functionalized Graphene Oxide in Enzyme Engineering: A Selective Modulator for Enzyme Activity and Thermostability. *ACS Nano* **2012**, *6*, 4864−4875.
(21) Saha, K.; Agasti, S. S.; Kim, C.; Li, X.; Rotello, V. M. Gold Nanoparticles in Chemical and Biological Sensing. *Chem. Rev.* **2012**, *112*, 2739−2779.
(22) You, C.-C.; Miranda, O. R.; Gider, B.; Ghosh, P. S.; Kim, I.-B.; Erdogan, B.; Krovi, S. A.; Bunz, U. H. F.; Rotello, V. M. Detection and Identification of Proteins Using Nanoparticle-Fluorescent Polymer 'Chemical Nose' Sensors. *Nat. Nanotechnol.* **2007**, *2*, 318−323.
(23) Aitha, M.; Marts, A. R.; Bergstrom, A.; Møller, A. J.; Moritz, L.; Turner, L.; Nix, J. C.; Bonomo, R. A.; Page, R. C.; Tierney, D. L.; Crowder, M. W. Biochemical, Mechanistic, and Spectroscopic Characterization of Metallo-β-Lactamase VIM-2. *Biochemistry* **2014**, *53*, 7321−7331.
(24) Champney, W. S.; Viswanatha, T.; Marrone, L.; Goodfellow, V.; Dmitrienko, G. Assays for beta-Lactamase Activity and Inhibition. In *Meth. Mol. Med.*; Humana Press: Totowa, NJ, 2008; Vol. *142*, pp 239−260.
(25) Wang, F.; Liu, J. Nanodiamond Decorated Liposomes as Highly Biocompatible Delivery Vehicles and a Comparison with Carbon Nanotubes and Graphene Oxide. *Nanoscale* **2013**, *5*, 12375−12382.
(26) Wang, F.; Liu, J. Liposome Supported Metal Oxide Nanoparticles: Interaction Mechanism, Light Controlled Content Release, and Intracellular Delivery. *Small* **2014**, *10*, 3927−3931.
(27) Zaki, A.; Dave, N.; Liu, J. Amplifying the Macromolecular Crowding Effect Using Nanoparticles. *J. Am. Chem. Soc.* **2012**, *134*, 35−38.
(28) Moali, C.; Anne, C.; Lamotte-Brasseur, J.; Groslambert, S.; Devreese, B.; Van Beeumen, J.; Galleni, M.; Frere, J.-M. Analysis of the Importance of the Metallo-β-Lactamase Active Site Loop in Substrate Binding and Catalysis. *Chem. Biol.* **2003**, *10*, 319−329.
(29) Borgianni, L.; Vandenameele, J.; Matagne, A.; Bini, L.; Bonomo, R. A.; Frere, J.-M.; Rossolini, G. M.; Docquier, J.-D. Mutational Analysis of VIM-2 Reveals an Essential Determinant for Metallo-β-Lactamase Stability and Folding. *Antimicrob. Agents Chemother.* **2010**, *54*, 3197−3204.
(30) De, M.; Ghosh, P. S.; Rotello, V. M. Applications of Nanoparticles in Biology. *Adv. Mater.* **2008**, *20*, 4225−4241.
(31) Shi, X.; Chang, H.; Chen, S.; Lai, C.; Khademhosseini, A.; Wu, H. Regulating Cellular Behavior on Few-Layer Reduced Graphene Oxide Films with Well-Controlled Reduction States. *Adv. Funct. Mater.* **2012**, *22*, 751−759.
(32) Frost, R.; Jonsson, G. E.; Chakarov, D.; Svedhem, S.; Kasemo, B. Graphene Oxide and Lipid Membranes: Interactions and Nanocomposite Structures. *Nano Lett.* **2012**, *12*, 3356−3362.
(33) Ang, P. K.; Jaiswal, M.; Lim, C. H. Y. X.; Wang, Y.; Sankaran, J.; Li, A.; Lim, C. T.; Wohland, T.; Barbaros, O.; Loh, K. P. A Bioelectronic Platform Using a Graphene-Lipid Bilayer Interface. *ACS Nano* **2010**, *4*, 7387−7394.
(34) Ip, A. C. F.; Liu, B.; Huang, P.-J. J.; Liu, J. Oxidation Level-Dependent Zwitterionic Liposome Adsorption and Rupture by Graphene-Based Materials and Light-Induced Content Release. *Small* **2013**, *9*, 1030−1035.
(35) Tu, Y. S.; Lv, M.; Xiu, P.; Huynh, T.; Zhang, M.; Castelli, M.; Liu, Z. R.; Huang, Q.; Fan, C. H.; Fang, H. P.; Zhou, R. H. Destructive Extraction of Phospholipids from *Escherichia coli* Membranes by Graphene Nanosheets. *Nat. Nanotechnol.* **2013**, *8*, 594−601.
(36) Lu, C. H.; Yang, H. H.; Zhu, C. L.; Chen, X.; Chen, G. N. A Graphene Platform for Sensing Biomolecules. *Angew. Chem., Int. Ed.* **2009**, *48*, 4785−4787.
(37) He, S. J.; Song, B.; Li, D.; Zhu, C. F.; Qi, W. P.; Wen, Y. Q.; Wang, L. H.; Song, S. P.; Fang, H. P.; Fan, C. H. A Graphene Nanoprobe for Rapid, Sensitive, and Multicolor Fluorescent DNA Analysis. *Adv. Funct. Mater.* **2010**, *20*, 453−459.
(38) Wu, M.; Kempaiah, R.; Huang, P.-J. J.; Maheshwari, V.; Liu, J. Adsorption and Desorption of DNA on Graphene Oxide Studied by Fluorescently Labeled Oligonucleotides. *Langmuir* **2011**, *27*, 2731−2738.
(39) Ruiz, O. N.; Fernando, K. A. S.; Wang, B. J.; Brown, N. A.; Luo, P. G.; McNamara, N. D.; Vangsness, M.; Sun, Y. P.; Bunker, C. E. Graphene Oxide: A Nonspecific Enhancer of Cellular Growth. *ACS Nano* **2011**, *5*, 8100−8107.
(40) Kempaiah, R.; Chung, A.; Maheshwari, V. Graphene as Cellular Interface: Electromechanical Coupling with Cells. *ACS Nano* **2011**, *5*, 6025−6031.

DOI: 10.1021/acsami.5b01954
ACS Appl. Mater. Interfaces 2015, 7, 9898−9903